PHYSICAL REVIEW
LETTERS

VOLUME 24 | 9 MARCH 1970 | NUMBER 10

EVIDENCE FOR COLLISIONLESS DAMPING OF UNSTABLE WAVES IN A MIRROR-CONFINED PLASMA*

C. C. Damm, J. H. Foote, A. H. Futch, Jr., A. L. Hunt, K. Moses, and R. F. Post
Lawrence Radiation Laboratory, University of California, Livermore, California 94550

and

J. B. Taylor
Culham Laboratory, Abingdon, England
(Received 12 January 1970)

Measurements of density thresholds for an ion-cyclotron instability in a mirror-confined plasma are interpreted in terms of a boundary for Landau damping of the unstable waves. Allowing for an observed normal-mode structure, experimental threshold values are accounted for quantitatively.

The collisionless damping of electrostatic plasma waves is expected to play an important role in achieving stable confinement of high-temperature plasmas. This Letter reports measurements of density thresholds for an ion-cyclotron instability in a mirror-confined plasma. The data support an interpretation of these thresholds as the densities above which electron Landau damping of the unstable plasma wave becomes too weak to suppress the instability. Malmberg and Wharton[1] have shown this damping mechanism to be in close quantitative agreement with the theoretical predictions of Landau[2] for the case of a uniform long plasma column with a Maxwellian electron distribution. The situation is somewhat different for a plasma in which energetic ions and lower-energy electrons are confined between magnetic mirrors. In this case the electrons are retained electrostatically, possessing a truncated Maxwellian distribution extending up to an energy corresponding to the positive ambipolar potential Φ_M. It is this limiting electron energy which apparently sets a bound on the operation of the Landau damping process in the present experiments.

Earlier experiments, both in the present apparatus[3] and in the "Phoenix II" experiment at Culham,[4] have demonstrated suppression of higher harmonics of the cyclotron instability when electrons were heated with microwaves. Transit-time heating of electrons is reportedly also effective in reducing normal rf emission in the Phoenix plasma.[5] These earlier qualitative indications of Landau damping in confined plasmas are reinforced and made quantitative by the measurements reported here.

The plasma is formed in a magnetic well by the injection of energetic hydrogen atoms and reaches a steady-state density for a period of several seconds. The experimental arrangement has been described previously, together with a description of some characteristics of the observed instability,[3] there identified as an ion-electron mode driven by the monoenergetic and anisotropic ion distribution.

To study the parametric dependence of the damping of the unstable waves, the instability-threshold densities have been measured over a

wide range of electron temperatures and ion energies. Experimentally, the instability threshold is determined in the following way: Correlated with each burst of rf activity at the ion gyrofrequency (indicating plasma instability) are abrupt temporary increases in the plasma potential resulting from the ejection of electrons. As the density is decreased by reducing the injected beam, the rf signals decrease in amplitude and become less frequent, finally dropping below the noise level of the detector. The potential variations remain detectable to a lower density, and the instability threshold density is defined by graphically extrapolating the observed burst rate to zero. Below this density there is no indication of unstable behavior on any detector and as far as can be determined the plasma is quiescent.

Two examples of threshold determinations are shown in Fig. 1. We have plotted densities in terms of the dimensionless parameter ϵ,

$$\epsilon \equiv \omega_{pi}^2/\omega_{ci}^2 \propto n^+ M_i/B^2, \quad (1)$$

where ω_{pi} and ω_{ci} are the ion plasma frequency and ion gyrofrequency, respectively, M_i is the ion mass, and B is the magnetic field. In Fig. 1(a) the threshold intercept is well defined and we can assign an error interval about the most probable intercept. In Fig. 1(b) we obtain, from a series of measurements with nearly constant operating conditions, a band of data points. The well-defined edges of this band yield two distinct values for the instability threshold. In each of four such cases both values are used in our analysis and, as will be seen below, a rationale appears for the dual threshold in terms of a normal-mode structure. (Data points lying between the edges of the band appear to represent average burst rates for a plasma which is alternating between the two modes.)

The plasma density is measured by turning off the beam and integrating the current of fast hydrogen atoms resulting from charge exchange during the plasma decay.[6] The secondary-electron-emission type of fast-atom detector was directly calibrated at several ion energies between 5 and 15 keV and the calibration was extended to 1 keV using a $W_i^{1/2}$ energy dependence[7] for the secondary-electron coefficient. The absolute density values found in this way are expected to be reliable to about ±30%.

As a measure of the maximum electron energy, the plasma potential is determined at each point by retardation measurement of the energy of slow ions formed by charge exchange and accelerated by the potential out through the mirrors. The magnitude of the potential depends upon the rate of collisional energy transfer from the hot ions to the electrons and upon the electron lifetime.[8] By adjusting the gas pressure in the plasma region and by varying the ion energy between 1 and 15 keV, the plasma potential was varied between 15 and 80 V.

The central value of magnetic field ranged between 1.3 and 6.2 kG, with proton orbit radius a_i varying from 1.6 to 3.6 cm. In all cases, the plasma boundary was at 30 cm axially and about 20 cm radially at the midplane.

In Fig. 2(a) we have plotted the threshold values of ϵ against $e\Phi_M/W_i$. A strong suggestion of a linear relation is apparent, and we have delineated an average boundary between the quiescent and unstable regions. However, in these threshold determinations there are clear variations from the average which are outside the error assignments.

An interpretation of these results can be made which describes the basic instability boundary and also in a plausible way accounts for the systematic variations in the threshold values and the "dual" thresholds typified by Fig. 1(b). We start with the assumption that the oscillations are basically electron plasma waves obeying a dispersion relation

$$\omega = n\omega_{ci} = \omega_{pe}(k_\parallel/k_\perp), \quad (2)$$

where $k_\parallel$ and $k_\perp$ are the components of the propgation vector. Equation (2) is derived from the infinite-medium dispersion relation[9] when the

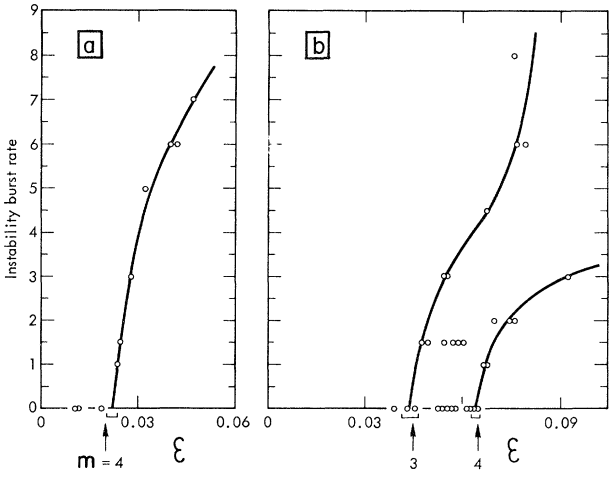

FIG. 1. Examples of experimental instability-threshold determinations. Arrows indicate predicted values from Eq. (8) for the assigned mode number, m.

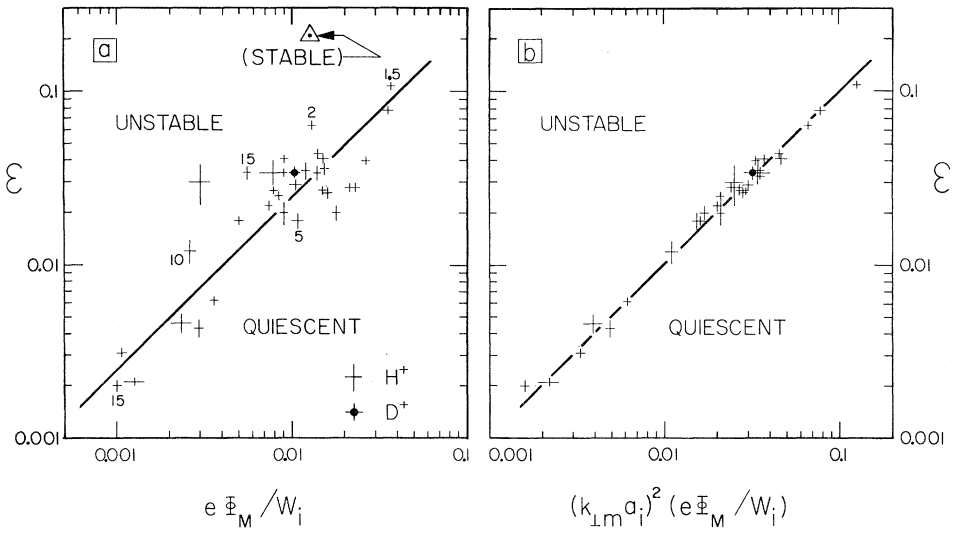

FIG. 2. (a) Values of ϵ at threshold for instability as a function of $e\Phi_M/W_i$. Length of lines forming crosses indicate estimated errors. Numbers near several points indicate values of W_i(keV). Point Δ is for a stable plasma decaying by charge exchange after a period of instability. (b) Comparison of measured values of ϵ and those predicted by Eq. (8).

ion terms are neglected and when $\omega/(k_\parallel \bar{v}_e)$ is large ($\bar{v}_e$ being the mean thermal velocity of the electrons). We are assuming here that Eq. (2) holds in the central region of our finite plasma. The threshold we have examined is for the fundamental, $n=1$. Additional calculations by one of the authors (R.F.P.), applying the differential equation for the perturbed potential in finite geometry, indicate that use of Eq. (2) is appropriate in the central region of the plasma.

Our second assumption is that the threshold for instability is the point at which electron Landau damping is no longer effective. In a situation with freely streaming electrons, strong Landau damping occurs when $\omega/k_\parallel$, the component of the phase velocity of the wave parallel to the magnetic field, locally matches the electron velocity, $v_\parallel$. In a confined plasma the analogous damping occurs when a harmonic of the electron bounce frequency ω_b matches the wave frequency ω. The difficulties in making a quantitative calculation of Landau damping in finite geometry have been pointed out by Cordey[10] and such a calculation is not available. However, we note that the bounce frequency requirement can usually be satisfied whenever there is a spread in bounce frequencies. In confined systems we postulate that even though the bounce resonance condition $\omega = N\omega_b$ may be satisfied, the local phase resonance condition is still dominant. That is, the damping will be small unless the local condition $\omega/k_\parallel = v_\parallel$ is also satisfied somewhere in the system.

The local resonance condition for Landau damping given above requires

$$\tfrac{1}{2}mv_\parallel^2 = \tfrac{1}{2}m(\omega_{pe}^2/k_\perp^2), \tag{3}$$

where we have used the dispersion relation, Eq. (2), and where ω_{pe} is the plasma frequency in the central region of the plasma. When the electrons are held in by an electrostatic potential as in the present experiments, then in the central region of the plasma there exists a range of possible electron energies given by

$$\tfrac{1}{2}mv_\parallel^2 \lesssim e\Phi_M. \tag{4}$$

From Eqs. (3) and (4) it follows that there can be no damping in the body of the plasma if

$$\tfrac{1}{2}m(\omega_{pe}^2/k_\perp^2) \gtrsim e\Phi_M. \tag{5}$$

Noting that $W_\perp \approx W_i$, we can rewrite Eq. (5) in the form

$$\epsilon \equiv \omega_{pi}^2/\omega_{ci}^2 \gtrsim (k_\perp a_i)^2 e\Phi_M/W_i, \tag{6}$$

which gives the value of ϵ above which damping vanishes in the central region.

For effective coupling between the ion gyromotion and the wave, $k_\perp a_i$ is expected to be approximately 2 for a δ-function ion distribution.[9,10] We can compare Eq. (6) directly with the experimental result of Fig. 2(a) since both ω_{pi} and ω_{ci} are determined for the central region of the plasma. The average experimental boundary line corresponds to $k_\perp a_i \approx 1.6$, with individual

values of $k_\perp a_i$ ranging between 1.1 and 3.2. The reasonable agreement between the expected and measured values of $k_\perp a_i$ indicates that the damping does indeed occur in the central region.

When the density exceeds the limit given by Eq. (6) there is still, in general, the possibility of wave damping in other regions of the plasma. As one approaches the ends of the system both the local wave velocity $v = \omega_{pe}/k_\perp$ and the limiting electron velocity must decrease. Whether or not there occurs the matching of velocities necessary for damping will depend upon the relation between the local plasma density and the local potential, in turn dependent on the electron velocity distribution. The situation is further complicated by the question of local wave reflection. If such reflection occurs inside the region of possible damping, it can prevent the wave damping from being effective. A recent theoretical discussion of these questions has been given by Berk.[11] The present experiment, which is compatible with damping in the central region, suggests that damping is ineffective in the outer regions of this particular plasma.

If Eq. (6) describes at least the average behavior, we can attempt to see more detail by assuming that this equation in fact describes the individual threshold values exactly. We measure all quantities at each data point except $k_\perp$, so a value of $k_\perp$ can be computed, with some error assignment. A distribution of measured $k_\perp$ values is then obtained by using a triangular weighting for each $k_\perp$ value within its error band and normalizing each triangle to unit area.

In the resulting histogram of combined $\ln k_\perp$ values, Fig. 3, a prominent quantization or mode structure of $k_\perp$ is evident. In the absence of a more refined finite-geometry calculation, we can reasonably fit the discrete set of values of $k_\perp$ suggested by Fig. 3 with a simple normal-mode model. Remembering that $k_\perp$ has both a radial and azimuthal component ($k_\perp^2 = k_r^2 + k_\theta^2$), we suggest that the radial eigenmode is single valued and that the azimuthal mode can be represented by $k_\theta = m/R$. Selecting $k_r = 0.25\ \mathrm{cm}^{-1}$ and $R = 6.9$ cm, we can write

$$k_{\perp m} = [(0.25)^2 + (m/6.9)^2]^{1/2}\ \mathrm{cm}^{-1}. \quad (7)$$

Values of $k_{\perp m}$ from Eq. (7) are noted on Fig. 3, from $m = 1$ to 6, and agree well, in general, with the experimental $k_\perp$ structure. While the numerical values for k_r and k_θ were selected to give this correspondence, the choices are reasonable when compared with plasma dimensions.

By making suitable assignments of $k_{\perp m}$ values, we can compare experimental threshold values for all data points with predicted thresholds ϵ', where

$$\epsilon' = (k_{\perp m} a_i)^2 e\Phi_M / W_i. \quad (8)$$

The result, plotted in Fig. 2(b), brings the data into nearly a statistical distribution about a mean line, $\epsilon = \epsilon'$. The dual thresholds of Fig. 1(b) now arise naturally from $k_{\perp 3}$ and $k_{\perp 4}$ assignments, and the corresponding predicted thresholds are indicated on Fig. 1(b). We should emphasize that the correspondence between predicted and observed thresholds arises from the $k_\perp$ structure observed, and is not dependent on the veracity of the simplified normal-mode description we have presented.

Values of $k_\parallel$ for the central region, calculated from the dispersion relation, Eq. (2), for each threshold measurement, extend from about 0.04 to 0.20 cm^{-1}. Perhaps coincidentally, the minimum corresponds to a half wavelength of 78 cm, which is close to the chamber length of 60 cm. Our data are inadequate to decide whether a quantization of $k_\parallel$ values also exists.

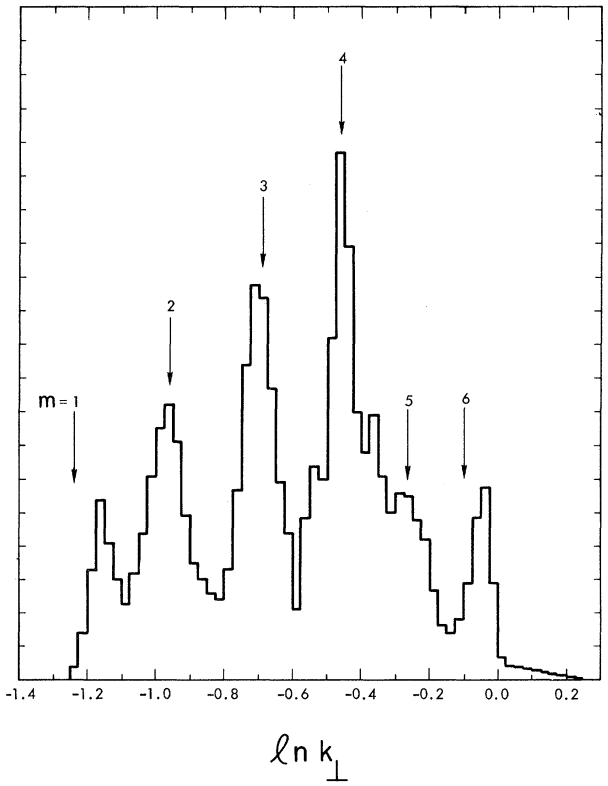

FIG. 3. Histogram showing the distribution of measured values of $\ln k_\perp$ ($k_\perp$ in cm^{-1}). Arrows indicate values of $\ln k_{\perp m}$ from Eq. (7).

The additional single point (Δ) plotted in Fig. 2(a) represents a stable plasma (decaying solely by charge exchange) observed when the injected beam was turned off after a period of violent instability. The plasma is typically stable during such decay periods even at densities well above the threshold line of Fig. 2 (see, for example, Fig. 3 of Ref. 3). A measured transient increase in electron energy during the decay[12] does not seem to be sufficient by itself to account for the large shift in stability level observed. The change in stability level may be attributed to a broadening of the trapped-particle distribution by the action of the instability. Evidence for the energy spreading of the ions under these conditions has been reported,[3] and one expects a similar smoothing of the angular and spatial distributions to occur. The observed enhanced stability could result from a reduced ion-driving term for the instability, from reduced wave reflections (allowing damping to occur in the outer regions of the plasma), or from a combination of these effects, including the transient increase in electron temperature.

In summary, the above interpretation of our threshold measurements accounts quantitatively for data taken over a wide range of experimental parameters. The results lend support to theories of wave-damping effects in mirror-confined plasmas.[11] These same theories point the way to the achievement of stably confined plasma at high density.

We wish to acknowledge the continued support and encouragement of C. M. Van Atta. We also thank H. L. Berk, T. K. Fowler, L. S. Hall, and L. D. Pearlstein for many stimulating discussions. F. Gordon and J. E. Osher helped to achieve the necessary beams at the various energies. The assistance of E. H. Dolstra and J. O. Ott in the operation of the experiment was invaluable.

---

*Work performed under the auspices of the U. S. Atomic Energy Commission.

[1]J. H. Malmberg and C. B. Wharton, Phys. Rev. Letters 13, 184 (1964).

[2]L. Landau, J. Phys. Radium 10, 45 (1946).

[3]C. C. Damm et al., in Proceedings of a Conference on Plasma Physics and Controlled Nuclear Fusion Research, Novosibirsk, U.S.S.R., 1968 (International Atomic Energy Agency, Vienna, Austria, 1969) Vol. II, p. 253.

[4]J. G. Cordey et al., in Proceedings of a Conference on Plasma Physics and Controlled Nuclear Fusion Research, Novosibirsk, U.S.S.R., 1968 (International Atomic Energy Agency, Vienna, Austria, 1969) Vol. II, p. 267.

[5]E. Thompson et al., Bull. Am. Phys. Soc. 13, 1520 (1968).

[6]C. C. Damm et al., Phys. Fluids 8, 1472 (1965).

[7]U. A. Arifov et al., Izv. Akad. Nauk. SSSR, Ser. Fiz. 26, 1403 (1962) [Bull. Acad. Sci. USSR, Phys. Ser. 26, 1427 (1963)].

[8]J. H. Foote, A. H. Futch, Jr., and C. C. Damm, Bull. Am. Phys. Soc. 13, 1520 (1968).

[9]L. S. Hall, W. Heckrotte, and T. Kammash, Phys. Rev. 139, A1117 (1965).

[10]J. G. Cordey, Phys. Fluids 12, 1506 (1969).

[11]H. L. Berk, Lawrence Radiation Laboratory Report No. UCID-15591, 1969 (unpublished).

[12]A. H. Futch, Jr. et al., Bull. Am. Phys. Soc. 14, 1054 (1969).

INVESTIGATION OF COLLECTIVE ELECTRON OSCILLATIONS IN Cd, Mg, AND Zn BY PHOTOEMISSION

B. Feuerbacher and B. Fitton
Surface Physics Division, European Space Research Organization, Noordwijk, Holland
(Received 19 December 1969)

The plasma resonance in films of Mg, Zn, and Cd, was measured by observing the associated peak in photoemission. For Mg, the plasmon energy of 10.21 eV and lifetime of 1.09×10^{-15} sec agree with values obtained by energy-loss and optical techniques. For Zn and Cd the plasmon energies are 9.46 and 8.68 eV, respectively. The lifetimes of 1.14×10^{-15} sec and 0.82×10^{-15} sec, for Zn and Cd, respectively, are considerably larger than previously observed.

The optically induced plasma resonance[1] provides a direct method of observing the collective oscillations of electrons in metals. Since the resonance is investigated by optical means, a high resolution is more easily obtained than by the earlier methods of observation which determined the discrete energy loss of fast electrons. The measurement of the optical constants from reflectivity data also allows the loss function to be calculated. Although using optical methods,